386. LINE SCALE COMPARATOR CARRIAGE VIBRATIONS DURING DYNAMIC CALIBRATION

A. Kasparaitis [1], V. Vekteris [2], A. Kilikevichius [3]
[1, 2, 3] Vilnius Gediminas Technical University,
Basanaviciaus str. 28, Vilnius, Lithuania
E-mail: [1] a.kasparaitis@bsp.lt, [2] vekteris@me.vtu.lt , [3] akilikevicius@gmail.com

(Received 8 March 2008, accepted 20 May 2008)

Abstract. Oscillations of the comparator, which is used for the dynamic calibration of long optical line scales, are analyzed in the paper. The accuracy of determination of the position of optical lines on the scale depends on the velocity of the carriage, which transports the microscope with a CCD camera in relation to the line scale. Oscillations influence the velocity equability, its value, and at the same time the error compo measuring. The base part of the comparator is acted upon by external excitations which come through the foundation and supports, also due to natural frequencies of the comparator set. It is shown in the work that vibration surroundings acting on the comparator have a random character and correspond to the criteria of the normal (Gauss) distribution. It is proved experimentally that preaching amplitudes of measured components of vertical and horizontal oscillations influence the stability of the carriage movement which causes the error of measuring.

Keywords: comparator, dynamic calibration, vibration, carriage, measuring, calibrated scale.

Introduction

Line gauges are important components in the length link chain. They are used in the measuring devices (systems) and technological equipment, etc.

The world practice witnesses increased focusing on the improvement of line gauge technologies and application thereof in length measurement and precise controlled motion systems. Modern precision scale production technologies enable to create small-step displacement transducers with measuring possibilities that come close to those of optical interferometers. Currently, line gauges with 0.125 nm (1,25 Å) resolution are used in precision devices [1, 2, 3].

A rapid advance of technologies, primarily micro- and nanotechnologies as well as micro-electro-mechanical system (MEMS) technologies raises higher and higher precision requirements, measuring speed requirements and other requirements thus stimulating creation of new precision length calibration systems. Reacting to these challenges the national metrology institutes (NMI) and manufacturing companies create new linear scale comparators whereof calibration uncertainty is a value of the nanometer range.

A line gauge defines one or several length values which are determined by the shortest distance between the centers of two lines of the periodic structure (scale).

Line gauges are calibrated by means of optical interference comparators with a sliding microscope for viewing scale lines and with a sliding measuring scale [4, 5, 6]. Interferometric measuring systems are used for precise measurement of the displacement of these sliding parts. Generally, the sources of interferometer stabilized frequency radiation are double-frequency He-Ne lasers.

A calibrated scale is precisely exposed under the microscope. Split-field photoelectric microscopes, point projection microscopes, confocal microscopes and photoelectric microscopes with CCD camera are used for the initial positioning and the positioning of the centers of lines of the measuring scale. The type of the microscope used determines in essence the measurement signal processing algorithm and the calibration precision and rate. Further details about line (edge) detection microscopes are presented in [4, 6].

Besides many device characteristics whereon scanning of line gauges of the comparator is dependent, external factors affect the precision of the device as well. One of the utmost effects is produced by vibrations. Lengthwise vibrations affect the carriage speed dynamics which directly affects the scanning precision.

The length of the calibrated end gauge and the position of line centers are precisely determined (calculated) by processing of the measurement data, by estimating the corrections of the environment conditions on the basis of pressure, humidity, temperature and CO_2 content measurement results. The lengths of the scale intervals obtained from the measuring system are recalculated for the 20 °C temperature.

The line gauge calibration procedures are determined by documents [7, 8].

Most dangerous are the vibrations that occur in the direction of the carriage motion (*x* axis) and torsional vibrations that occur on the carriage axis *z* (on *x, y* plane) which is perpendicular to the direction of motion *x*. Vibrations that occur in the direction of the length of the carriage, i.e. the carriage velocity and its dynamics determine the precision of scanning of the line gauge position. Precision is defined by means of a photoelectric microscope with a CCD camera.

Object of research.

An interference comparator with air refraction coefficient compensation meets the technical and economic criteria by estimating the refraction coefficient from Edlen formula according to the results of measurement of the environment parameters or by means of a refractometer. The structural diagram of the equipment is shown in Fig. 1. It is based on a line gauge calibration comparator with a sliding microscope and a stationary scale. The comparator's frame is made from granite and is mounted on vibration-proof supports, the microscope holder moves on air guides. The carriage is driven by means of motor, worm reduction gear and friction gear. The laser measuring system comprises laser, interferometer and retroreflector.

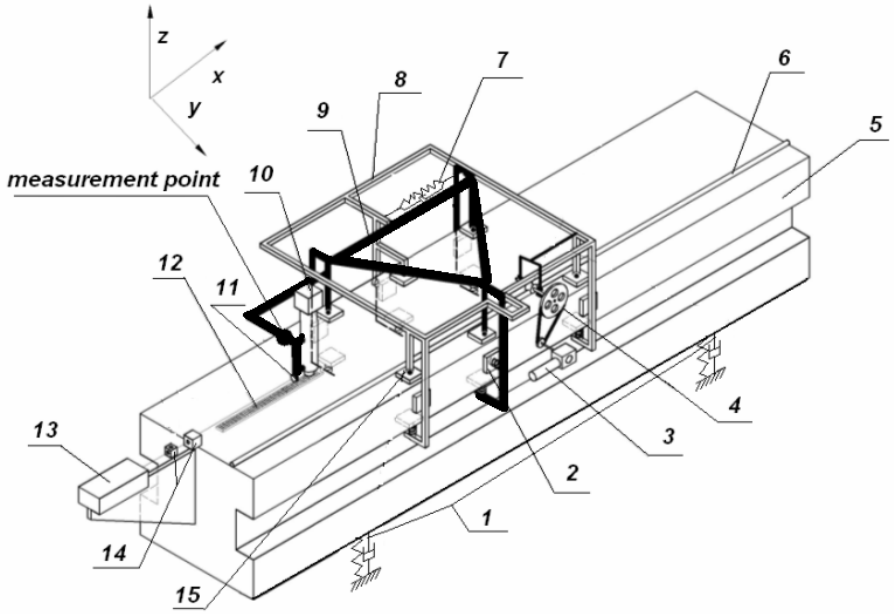

Fig.1. A structural diagram of the comparator: 1 - vibration insulation supports; 2 – springy aerostatic bearing; 3 – electromotor with reducer; 4 – belt drive; 5 – granite guideway; 6 – friction gear; 7 – joint member of two carriage; 8 – frame of force carriage; 9 – frame of the precision carriage; 10 – microscope with camera and flash; 11 – retroreflektor; 12 – calibrate scale; 13 – laser head; 14 – linear interferometer; 15 –tight built aerostatic bearing

Dynamical model of the comparator

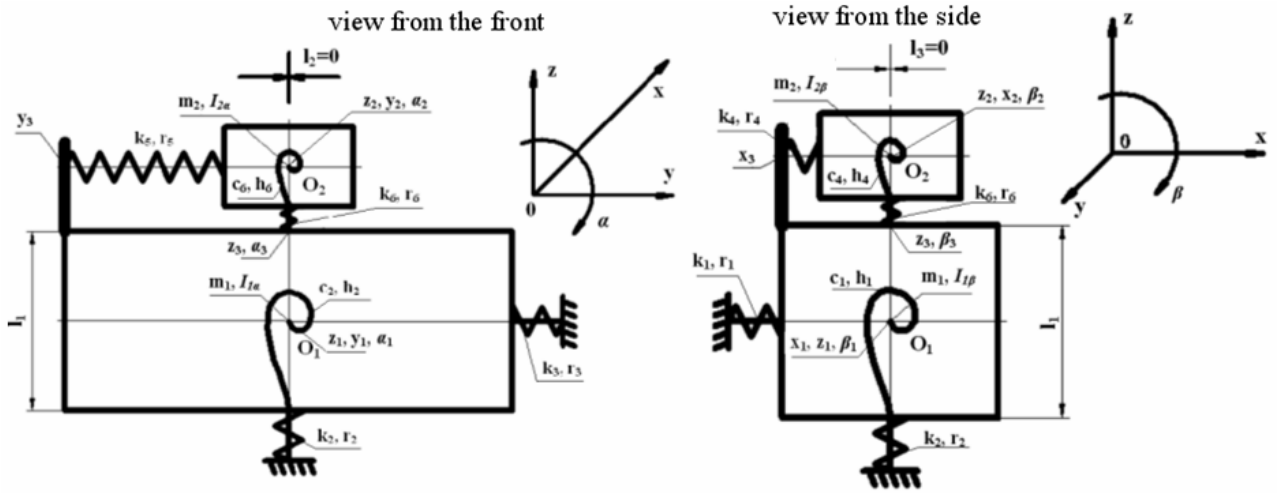

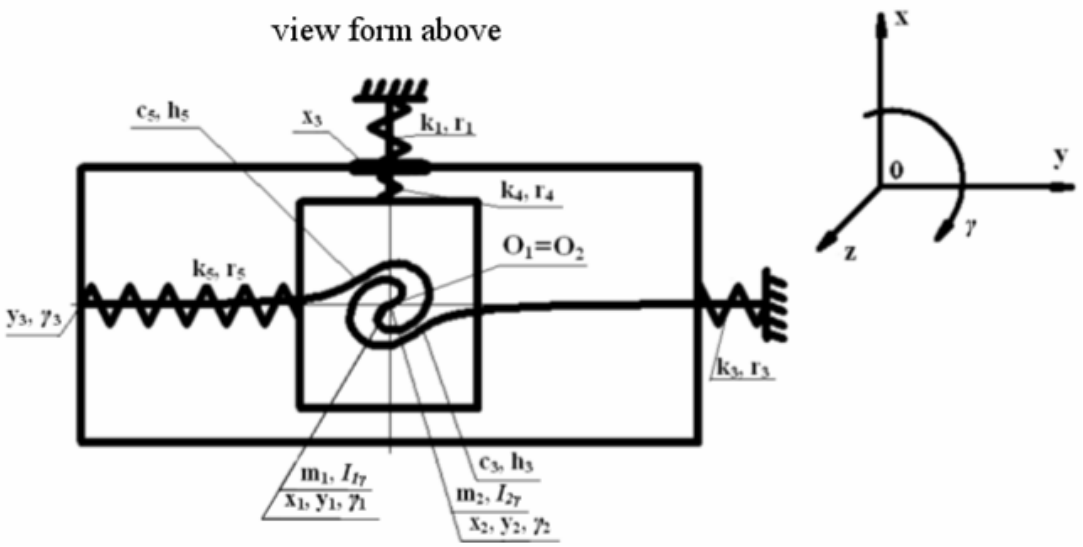

Fig. 2. Dynamical model of the comparator

There O_1, O_2 – center of masses; m_1, m_2 – are masses of assembly units; I_{1j}, I_{2j}, inertia moments, where j – coincides with angles α, β, γ;

Stiffness coefficients k_n – is of linear motion; c_n – is of angular rotation motion (n=1,..., 6). Damping coefficients r_n – is of linear motion; h_n – is of angular rotation motion (n=1,...,6).

For equation forming simplification the dynamic model at a comparator we are dividing into two subsystems: the 1–st subsystem consists of vibration insulation supports without connection with a carriage; the 2–nd subsystem consists of carriage with ties connecting it with the bed of granite.

The main coordinates of two subsystem are x_i, y_i, z_i, α_i, β_i, γ_i (i=1, 2) which fix linear and angular motions of mass centers in coordinate systems with initial position in points O_1 and O_2. All members of coordinates are 12 main ones and 6 additional: x_3, y_3, z_3, α_3, β_3, γ_3.

To research vibration of 12 degree of freedom systems is mostly compact at using matrices. A vibration of the system is mostly convenient to describe by matrix:

$$[A]\{\ddot{q}\}+[B]\{\dot{q}\}+[D]\{q\}=\{Q(t)\} \qquad (1)$$

There [A], [B], [D] are generalized inertia, damping and stiffness coefficients of matrices; $\{q\}, \{\dot{q}\}, \{\ddot{q}\}$ are generalized coordinates of displacement, velocity and acceleration one columns matrices; $\{Q(t)\}$ – external generalized force column acting in accordance with force:

$$[A]=\begin{bmatrix} a_{11} & a_{12} & \dots & a_{112} \\ a_{21} & a_{22} & \dots & a_{212} \\ \vdots & \vdots & \vdots & \vdots \\ a_{121} & a_{122} & \dots & a_{12 12} \end{bmatrix}$$

$$[B]=\begin{bmatrix} b_{11} & b_{12} & \dots & b_{112} \\ b_{21} & b_{22} & \dots & b_{212} \\ \vdots & \vdots & \vdots & \vdots \\ b_{121} & b_{122} & \dots & b_{12 12} \end{bmatrix} \qquad (2)$$

$$[D]=\begin{bmatrix} d_{11} & d_{12} & \dots & d_{112} \\ d_{21} & d_{22} & \dots & d_{212} \\ \vdots & \vdots & \vdots & \vdots \\ d_{121} & d_{122} & \dots & d_{12 12} \end{bmatrix}$$

$$\{q\}=\begin{Bmatrix} q_1 \\ q_2 \\ \vdots \\ q_{12} \end{Bmatrix}; \{\dot{q}\}=\begin{Bmatrix} \dot{q}_1 \\ \dot{q}_2 \\ \vdots \\ \dot{q}_{12} \end{Bmatrix};$$

$$\{\ddot{q}\}=\begin{Bmatrix} \ddot{q}_1 \\ \ddot{q}_2 \\ \vdots \\ \ddot{q}_{12} \end{Bmatrix}; \{Q(t)\}=\begin{Bmatrix} Q_1(t) \\ Q_2(t) \\ \vdots \\ Q_{12}(t) \end{Bmatrix} \qquad (3)$$

Expression at kinetic and potential energy and dissipative function it is possible to write as a product of row matrix and one columns matrix:

$$T = \frac{1}{2}\{\dot{q}\}^T [A]\{\dot{q}\};$$
$$\Pi = \frac{1}{2}\{q\}^T [D]\{q\}; \quad (4)$$
$$\Phi = \frac{1}{2}\{\dot{q}\}^T [B]\{\dot{q}\};$$

There [*A*], [*B*], [*D*] are generalized inertia, damping and stiffness coefficients square 12 members matrix; $\{q\}$, $\{\dot{q}\}$ are one columns matrices and their differential; $\{q\}^T$, $\{\dot{q}\}^T$ are one row matrices of generalized coordinates and their differential.

When a dynamic model is obtained (Fig. 2) a mathematical model of the tested system is created (vibration equation). To this end Lagrange's equation of the second type is used [9]:

$$\frac{d}{dt}\left(\frac{dT}{d\dot{q}_i}\right) - \frac{dT}{dq_i} + \frac{d\Phi}{d\dot{q}} + \frac{d\Pi}{dq_i} = Q_i(t) \quad (5)$$

There T, Π are the system's kinetic and potential energy;
Φ – dissipation function;
q_i – i-th generalized coordinate;
$Q_i(t)$ – generalized force acting in accordance with coordinate q_i.

At forming of equation lat we use expressions of T_i and Π_i (i=1, 2) presented in formula 6.

$$2T_i = m_i\left(\dot{x}_i^2 + \dot{y}_i^2 + \dot{z}_i^2\right) + I_{i\alpha}\dot{\alpha}_i^2 + I_{i\beta}\dot{\beta}_i^2 + I_{i\gamma}\dot{\gamma}_i^2; \quad (\mathrm{i} = 1, 2)$$
$$2\Pi_1 = k_1(x_1 - x_0)^2 + k_3(y_1 - y_0)^2 + k_2(z_1 - z_0)^2 + c_2(\alpha_1 - \alpha_0)^2 + c_1(\beta_1 - \beta_0)^2 + c_3(\gamma_1 - \gamma_0)^2 \quad (6)$$
$$2\Pi_2 = k_4(x_2 - x_3)^2 + k_5(y_2 - y_3)^2 + k_6(z_2 - z_3)^2 + c_5(\alpha_2 - \alpha_3)^2 + c_4(\beta_2 - \beta_3)^2 + c_6(\gamma_2 - \gamma_3)^2$$

There x_0, y_0, z_0, α_0, β_0, γ_0 are excitations of a bed with consequent coordinates. View at dissipation function (Φ_i) is received from Π_i, after changing stiffness coefficients to damping coefficients. Connecting equations are expressed: $x_3 - x_1 - l_1\beta_1 - l_2\gamma_2 = 0$; $y_3 - y_1 - l_1\alpha_1 - l_3\gamma_1 = 0$; $z_3 - z_1 - l_2\alpha_1 + l_3\beta_1 = 0$; $\alpha_3 - \alpha_1 = 0$; $\beta_3 - \beta_1 = 0$; $\gamma_3 - \gamma_1 = 0$;
After performing modeling by means of Matlab 6.1 and Origin 6.1 software packages we obtain the results presented in Fig. 3.

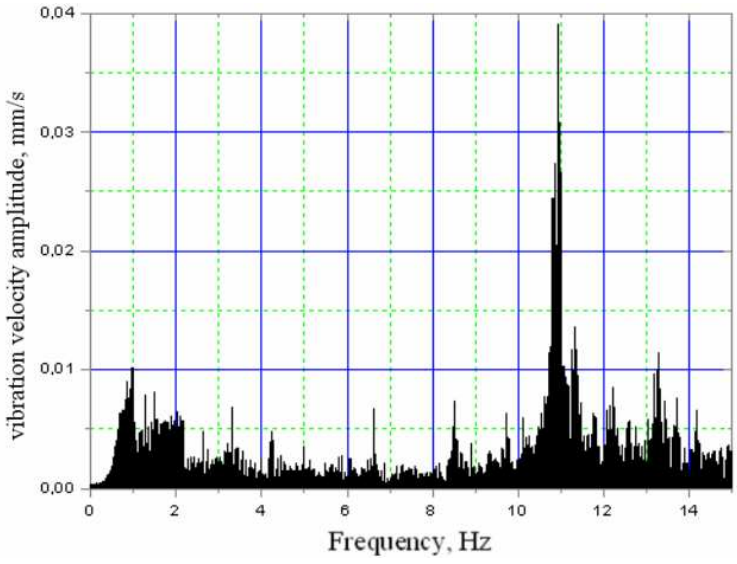

Fig. 3. Spectrum of the vibration velocity (during dynamic calibration)

Experimental tests

Experimental tests were conducted in measurement point shown in Fig. 1. To this end a measuring system (Fig. 4) was installed comprising an accelerometer 8306, vibrometer 2511, signal input and control board Ebiol–Comlab–SeiTech and personal computer IBM–50 [10, 11, 12, 13]. The obtained results are presented in Figs. 4–8.

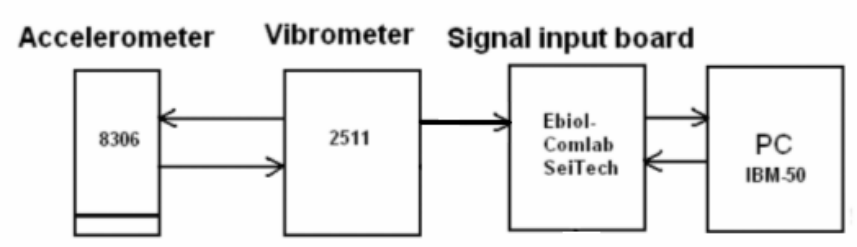

Fig. 4. Flow chart of diagnostic measurements

The measurement point with the precision carriage being in a static position (without air supplying).

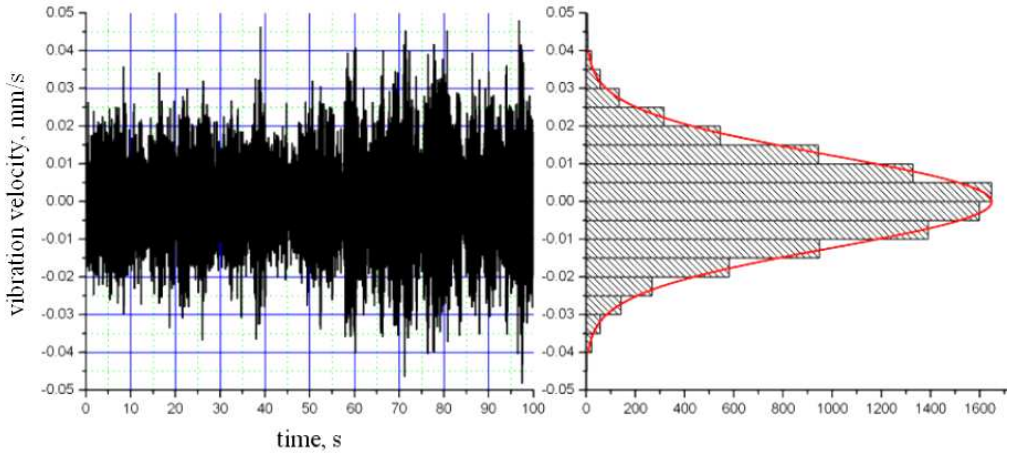

Fig. 5. The signal of the vibration velocity and its histogram

Table 1 Statistical parameters of the vibration velocity measurement signal

Statistical parameter	Arithmetical mean, [mm/s]	Root mean square deviotion	Minimum value, [mm/s]	Maximum value, [mm/s]	Scatter, [mm/s]
Value	-3.123E-6	0.01224	-0.04807	0.04795	0.09601

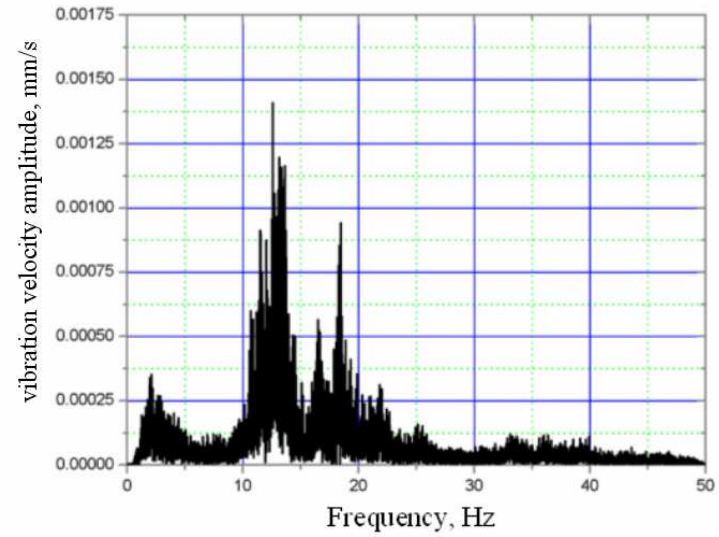

Fig. 6. The spectrum of the vibration velocity signal (without air supplying)

The measurement point with the precision carriage being in a static position (with air supplying).

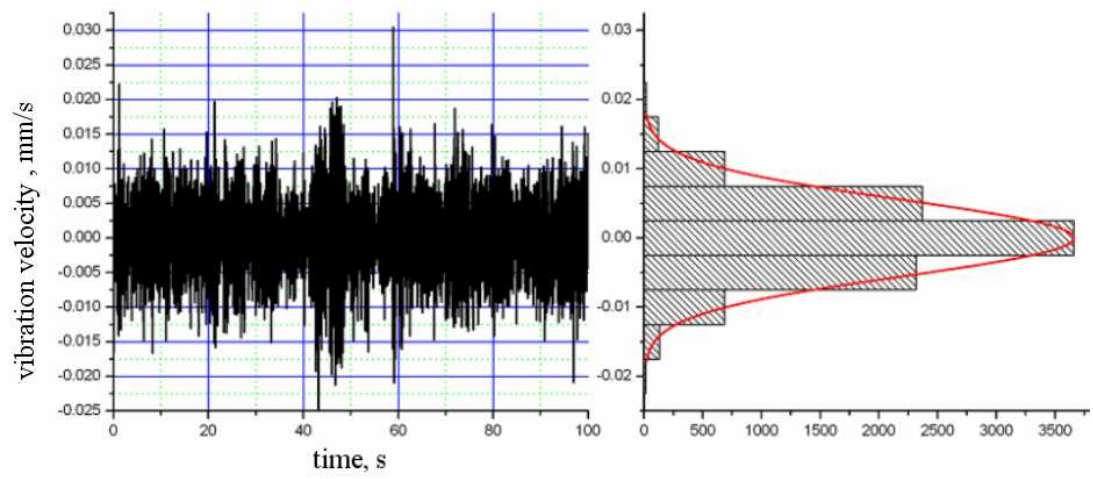

Fig. 7. The signal of the vibration velocity and its histogram

Table 2 Statistical parameters of the vibration velocity measurement signal

Statistical parameter	Arithmetical mean, [mm/s]	Root mean square deviotion	Minimum value, [mm/s]	Maximum value, [mm/s]	Scatter, [mm/s]
Value	2.882E-6	0.00549	-0.02623	0.0305	0.05673

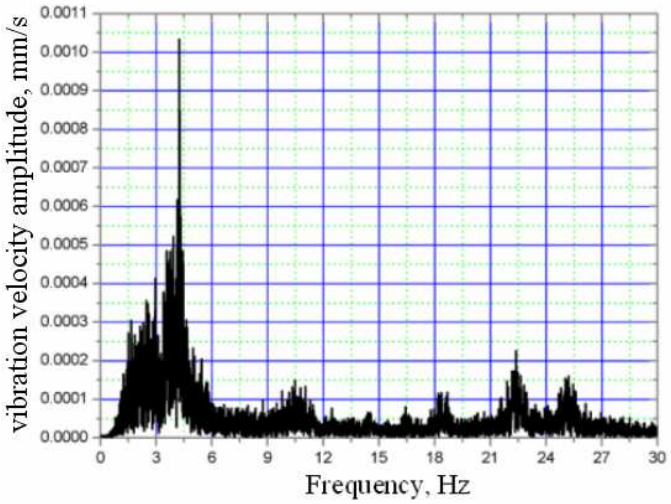

Fig. 8. The spectrum of the vibration velocity signal (with air supplying)

The measurement point during dynamic calibration

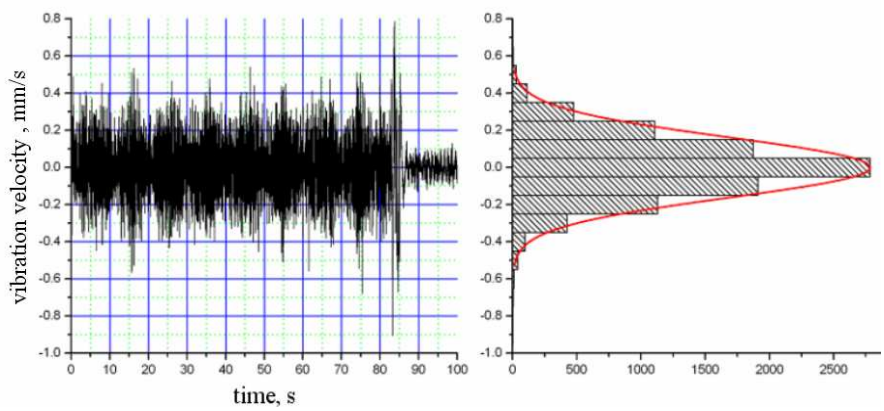

Fig. 9. The signal of vibration velocity and its histogram

Table 3. Statistical parameters of the vibration velocity measurement signal

Statistical parameter	Arithmetical mean, [mm/s]	Root mean square deviotion	Minimum value, [mm/s]	Maximum value, [mm/s]	Scatter, [mm/s]
Value	2.8118E-4	0.16196	-0.90585	0.7869	1.69275

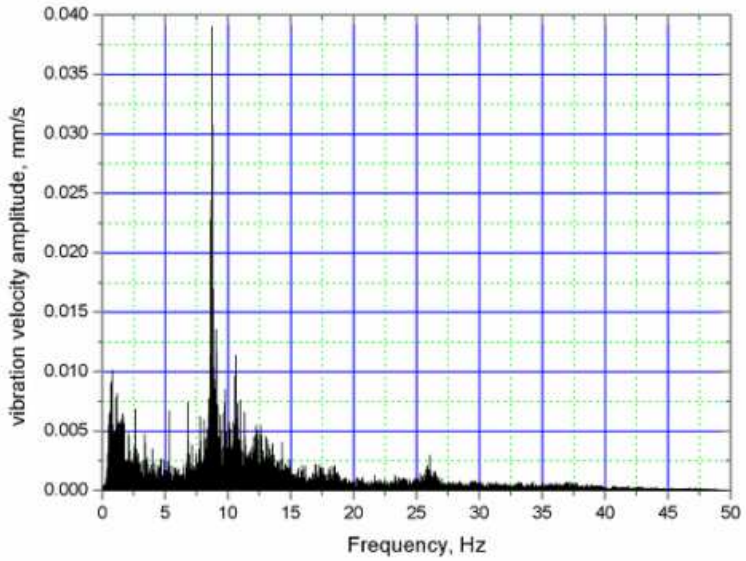

Fig . 10. The spectrum of the vibration velocity signal (during dynamic calibration)

Discussion of the results

Measurements were carried out in horizontal directions. Supply of air to the comparator's frame supports and the carriage's aerostatic bearings was controlled. The illustrations show the measurement point at which vibration velocity amplitudes reach maximum values at the respective frequencies.

The obtained experimental results show that the amplitudes of vibration velocity level at 0,1 – 0,4 mm/s (without air supplying) decrease at 0,05 – 0,15 mm/s. The vibration velocities during dynamic calibration fluctuate from 0,2 to 0,4 mm/s. The obtained experimental results show that the spectral amplitudes of vibration velocity (without air supplying) at 10 – 20 Hz frequencies fluctuate from $0{,}5\cdot10^{-3}$ to $1{,}4\cdot10^{-3}$ mm/s, whereas at other frequencies vibration velocity amplitudes are inconsiderable. The spectral amplitudes of vibration velocity (with air supplying) at 1 – 6 Hz frequencies fluctuate from $0{,}3\cdot10^{-3}$ to $1{,}05\cdot10^{-3}$ mm/s, whereas at other frequencies vibration velocity amplitudes are inconsiderable. The spectral amplitudes of vibration velocity during dynamic calibration at 8 – 10 Hz frequencies fluctuate from 0,015 to 0,040 mm/s.

Results obtained in theoretical tests are markedly expressed at 10 – 12 Hz frequencies only, where amplitudes reach up to 0,040 mm/s. This is related to inaccurate setting of parameters of differential equations. Hence, result reliability problems arise in the course of determining the vibration level of such accurate calibration devices by calculating methods. Therefore, to find out possible sources of uncertainties and errors in the course of creating tools of such high-end technologies one should be guided by experimental tests despite the fact of their expensive costs.

Conclusions

Such experimental results are received on the ground of dynamic mathematical models:

1. Where the comparator's calibration uncertainty is 0,1 μm/m the obtained values of vibration velocitys may affect the accuracy of reading.
2. The spectra of random vibration velocitys obtained within the low-frequency range (2 – 10 Hz) define the preparation requirements of the vibration-proof supports.
3. These vibration velocities are acting and must be measured setting the accuracy of raster indication.

REFERENCES

[1] Thalmann R. *A new High Precision Length Measuring Machine, Progress in Precision Engineering and Nanotechnology* (Proceedings of the 9-IPES/UME4, Braunschweig, Germany, 1997, Vol.1, pp. 112-115).

[2] Demarest F. C. *High-resolution, high-speed, low data age uncertainty, heterodyne displacement measuring interferometer electronics* (Meas. Sci. Technol. 9 (1998), P. 1024-1030).

[3] Beers J. S., Penzes W. B. *The NIST Length Scale Interferometer* (J. Res. Natl. Inst. Stand. Technol. 104, 225 (1999)).

[4] NANO 3: *Line Scale Standards, WGDM-7, Preliminary comparison on nanometrology according to the rules of CCL*

key comparisons (FINAL REPORT, Braunschweig, August 29, 2003, p. 119).

[5] Nano4: *1D gratings, WGDM-7: Preliminary comparison on nanometrology according to the rules of CCL key comparisons* (Final report, Draft B, Wabern, 30. November 2000, p. 34).

[6] *Creation and Research into Precision Length Calibration Systems* (2003 Report on the VMSF Research Program Reg. No B-03008, Kaunas 2003, p. 181).

[7] *EUROMET Guidelines on Conducting Comparisons EUROMET* (Guide No 3 Issued: 08.12.1998 Revised: 08.05.2002/Sa Version: 02.7b, p.6).

[8] EUROMET Guidelines on Conducting Comparisons

[9] Vibrations in engineering. //Reference book in 6 volumes. Vol. 1/ Edited by V.V. Bolotin, M.: Machine-building, 1978, 352 p.

[10] Kilikevičius A., Vekteris V. *Vibrations Sources Acting the Comparator Stand* (Mechanika 2006 Proceedings of the 11th international conference. Kaunas 2006).

[11] Kilikevičius A., Vekteris V. *Diagnostic testing of the comparator carriage vibrations* (Ultragarsas Nr. 2(59). 2006).

[12] Vekteris V., Kilikevičius A. *Research of vibrations acting the mechatronical comparator* (Zbornik 4. simpozijuma sa medunarodnim učeščem „KOD 2006“ Zbornik Radova Proceedings. Palič 2006).

[13] Kasparaitis A., Vekteris V., Kilikevičius A. *A Vibration Source in Comparator* (Seventh International Conference on Vibration Measurements by Laser Techniques: Advances and Applications Vol.6345. Ancona, Italy, 2006).